Supplementary Information (SI) for Analyst.

Supporting Information

An Indolizine-derived Chemodosimeter with Enhanced Emission in Micellar Environment for ppb-level Detection of Mercury Ions

Amanda Ana Pinheiro[#], Ankit Thakuri[#], Soumik Saha, Mainak Banerjee*, Amrita Chatterjee*

Department of Chemistry, Birla Institute of Technology and Science Pilani, KK Birla Goa Campus,

Goa 403726, India

[#] authors contributed equally

Table of Contents

1. Experimental details

Chemicals and reagents

Cinnamaldehyde and 2-mercaptoethan-1-ol were purchased from SD Fine, 2-benzoylpyridinre and ethane-1,2-dithiol was purchased from Alfa, and boron trifluoride diethyl etherate was procured from SIAL, India. All other chemicals and solvents utilized in the study were obtained from various commercial suppliers. The chemicals were of analytical grade and were used directly without undergoing any additional purification steps.

Instrumentation, measurements and methods

All fluorescence measurements were carried out using a JASCO FP-8500 spectrofluorometer with an excitation wavelength set at 400 nm, and emission spectra were recorded in the range of 405–750 nm. The slit width was kept at 2.5 nm for both excitation and emission measurements. Infrared (IR) spectra were obtained using an IR Affinity-1 FTIR Spectrophotometer (Shimadzu). UV-vis spectra were acquired utilizing a JASCO V–550 spectrophotometer with a bandwidth and data pitch set at 1 nm. The NMR spectra were obtained using a Bruker Avance Neo 500 MHz spectrometer. A Triple Quadrupole LC/MS (model 6460) was used to obtain the ESI-MS spectra.

*Synthesis of 1,3-diphenylindolizine-2-carbaldehyde (**DPIC-CHO**)*[1]

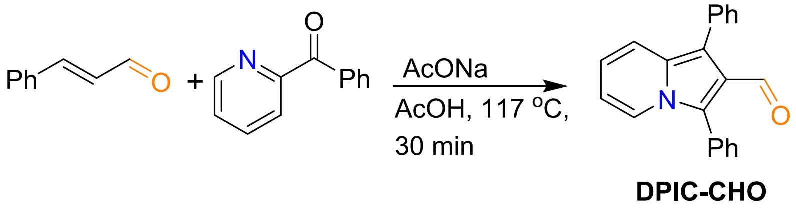

Scheme S1: Synthesis of **DPIC-CHO**

DPIC-CHO was synthesized via cycloaddition of cinnamaldehyde and 2-benzoyl pyridine via a reported procedure. [1] Briefly, a mixture of 2-benzoylpyridine (366 mg, 2 mmol), cinnamaldehyde (792 mg, 6 mmol) and sodium acetate (492 mg, 6 mmol) in acetic acid (25 mL) was taken in a round-bottomed flask and heated under reflux for 30 min. The reaction was cooled to room temperature, diluted with water and extracted using ethyl acetate. The organic layer was evaporated under reduced pressure to obtain crude product and purified via column chromatography to obtain **DPIC-CHO** (white solid, 368 mg, 70%). ^{1}H NMR (500 MHz, $CDCl_3$): δ (ppm) 10.01 (s, 1H), 7.87 (d, J = 7.5 Hz, 1H), 7.53-7.49 (m, 8H), 7.44 (t, *J* = 7.6 Hz, 2H), 7.35 (t, *J* = 7.6 Hz, 1H), 6.72 (t, *J* = 6.4 Hz, 1H), 6.53 (t, *J* = 6.9 Hz, 1H); ^{13}C NMR (125 MHz, $CDCl_3$): δ (ppm) 188.6, 133.1, 131.1, 130.7, 130.7, 130.3, 129.2, 129.1, 129.0, 128.3, 126.9, 122.7, 122.0, 119.7, 119.5, 116.3, 113.5.

Synthesis of probes

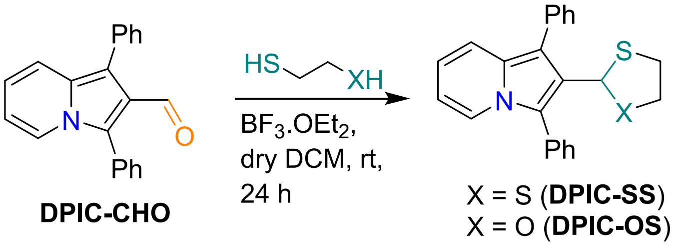

Scheme S2: Synthesis of **DPIC-SS** and **DPIC-OS**.

*2-(1,3-Dithiolan-2-yl)-1,3-diphenylindolizine (**DPIC-SS**)*

In a 10 mL round-bottom flask, **DPIC-CHO** (0.2 mmol) and ethane-1,2-dithiol (0.4 mmol) were dissolved in 4 ml dry dichloromethane, followed by dropwise addition of $BF_3.OEt_2$ (0.4 mmol). The reaction mixture was stirred at room temperature for 24 h. The organic layer was then washed with water and brine, dried over anhydrous Na_2SO_4, concentrated under vacuum, and purified using column chromatography to obtain pure **DPIC-SS**.

White solid, 51 mg (69%); ^{1}H NMR (500 MHz, $CDCl_3$): δ (ppm) 7.70 (d, *J* = 7.1 Hz, 1H), 7.62-7.59 (m, 4H), 7.51 (t, *J* = 7.6 Hz, 2H), 7.43 (t, *J* = 7.4 Hz, 3H), 7.31 (t, *J* = 6.7 Hz, 2H), 6.61 (t, *J* = 6.3 Hz, 1H), 6.38 (t, *J* = 6.8 Hz, 1H), 5.89 (s, 1H), 3.08-3.03 (m, 2H), 3.01-2.96 (m, 2H); ^{13}C NMR (125 MHz, $CDCl_3$): δ (ppm) 135.1, 131.70, 131.3, 131.2, 130.2, 128.7, 128.3, 128.1, 126.3, 123.5, 122.2, 122.0, 118.0, 117.8, 114.8, 111.1, 48.0 40.7; HRMS (ESI-TOF): *m/z* calcd for $C_{23}H_{20}NS_2$ $[M+H]^+$, 374.1037; found, 374.1033.

*2-(1,3-Oxathiolan-2-yl)-1,3-diphenylindolizine (**DPIC-OS**)*

A similar procedure was utilized for the synthesis of **DPIC-OS** was adopted from **DPIC-CHO** (0.2 mmol) using 2 equiv each of 2-mercaptoethan-1-ol and $BF_3.OEt_2$.

White solid, 43 mg (61%); ^{1}H NMR (500 MHz, $CDCl_3$): δ (ppm) 7.73 (d, *J* = 7.2 Hz, 1H), 7.59-7.52 (m, 5H), 7.48-7.44 (m, 4H), 7.33 (t, *J* = 7.5 Hz, 2H), 6.66 (t, *J* = 6.3 Hz, 1H), 6.43 (t, *J* = 6.8 Hz, 1H), 5.18 (s, 1H), 2.69-2.65 (m, 2H), 2.58-2.53 (m, 2H); $^{13}C\{^1H\}$ NMR (125 MHz, $CDCl_3$): δ (ppm) 134.7, 131.3, 131.0, 130.9, 129.0, 128.8, 128.5, 128.1, 126.8, 123.6, 122.8, 122.4, 118.2, 118.1, 114.0, 111.4, 60.7, 45.3, 37.1; HRMS (ESI-TOF): *m/z* calcd for $C_{23}H_{19}NOS$ $[M+H]^+$, 358.1266; found, 358.1267.

Procedure for fluorimetric studies

A 1 mM stock solution of Hg^{2+} ions was prepared in deionized water and utilized for all fluorimetric studies. The sensing ensemble contained 10 µL **DPIC-SS** (1 mM in DMSO) taken in an aqueous solution of CTAB (1 mM, 1 mL). To detect mercury ions, an increasing volume of an aqueous solution of Hg^{2+} ions was added to the sensing solution, keeping the volume constant (1 mL). The solution was incubated for 5 min before checking the fluorescence output. To evaluate the selectivity of sensing assay towards Hg^{2+} ions, stock solutions of various cations and anions (1 mM) were prepared in water. The stock solutions of neutral molecules (1 mM) were prepared either in water or EtOH-water (1:9). All studies were performed at room temperature and triplicated, and the average data was reported. Likewise, similar fluorimetric studies were performed, except the sensing ensemble contained 10 µL Probe **DPIC-OS,** and the solution showed a fluorimetric response after 2 min.

Procedure for UV-Vis studies

A similar procedure as above was adapted for UV-Vis studies.

Real sample analysis

For real sample analysis, water samples from various sources such as tap, sea, river, field, pond, and rain were collected. **DPIC-SS** and **DPIC-OS** were separately added to real water samples. The mixture was spiked with known concentrations of Hg^{2+}, and the final volume was made up to 1 mL by adding actual water samples and subjected to fluorimetric evaluation.

DFT calculations

The density functional theory (DFT)[2] was used to carry out theoretical studies, and for the time-dependent density functional theory (TD-DFT)[3-5] level, the Gaussian 09 program was used.[6] Becke's three-parameter exchange function (B3) with the Lee-Yang-Parr correlation (LYP) function was employed using a 6-31G basis set for optimizing molecular geometries.

2. Absorbance and emission spectra of DPIC-CHO, DPIC-SS and DPIC-OS in different organic solvents

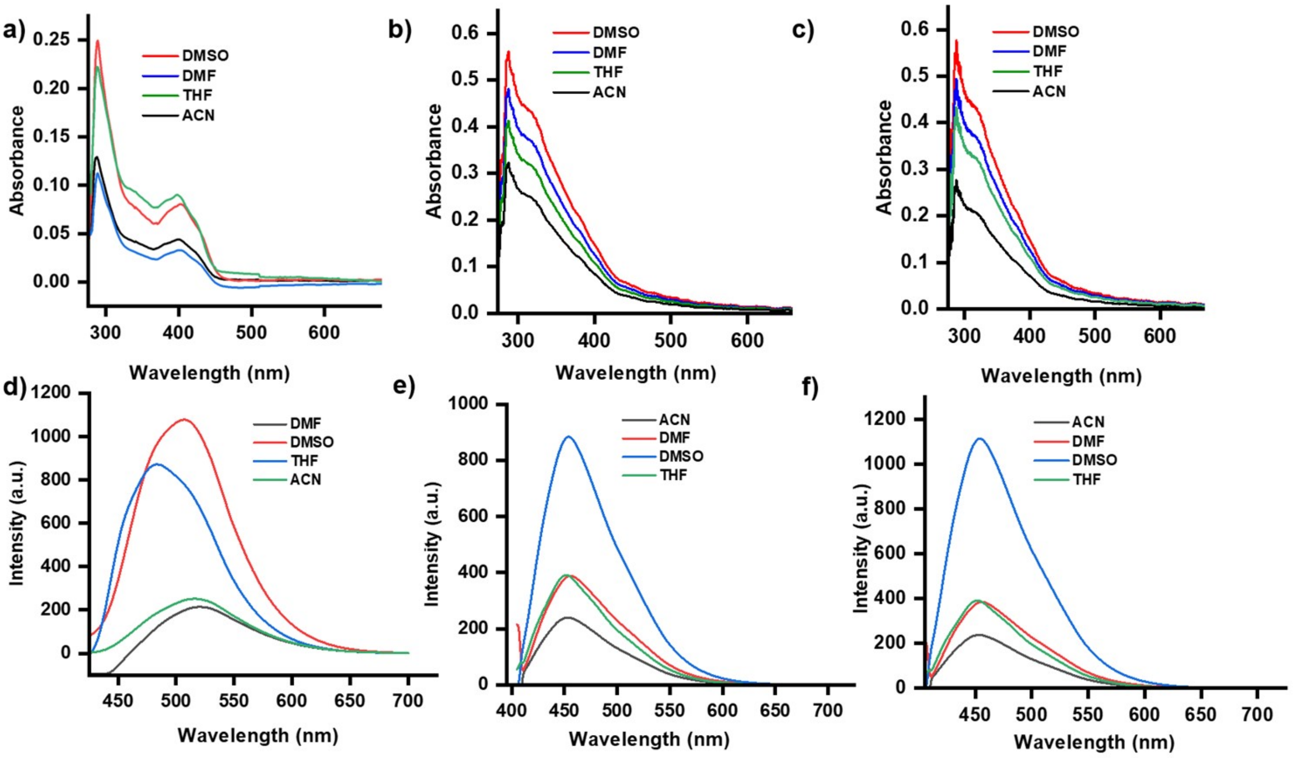

Figure S1. The UV-Vis spectra of a) **DPIC-CHO**, b) **DPIC-SS** and c) **DPIC-OS** in different solvents. The fluorescence spectra of d) **DPIC-CHO**, e) **DPIC-SS**, and f) **DPIC-OS** in different organic solvents. The study indicates that DMSO is the ideal solvent choice for fluorescence.

3. Table S1: Comparative photophysical studies of DPIC-OS and DPIC-SS in organic different solvents

DPIC-SS	λ_{abs} (nm)	λ_{em} (nm)	Intensity	Stokes shift (nm)	ΔE (J)	φ
DMF	285	454	384	169	1.18×10^{-18}	31
THF	275	452	391.02	177	1.12×10^{-18}	13
ACN	288	454	240.22	166	1.20×10^{-18}	20
DMSO	289	457	894.27	168	1.18×10^{-18}	39

DPIC-OS	λ_{abs} (nm)	λ_{em} (nm)	Intensity	Stokes shift (nm)	ΔE (J)	φ
DMF	278	452	384	174	1.14×10^{-18}	20
THF	286	452	391.02	166	1.20×10^{-18}	23
ACN	297	454	240.22	157	1.27×10^{-18}	15
DMSO	288	453	1110.27	165	1.20×10^{-18}	36

4. Ths UV-Vis and fluorescence studies of DPIC-SS and DPIC-OS in micellar media

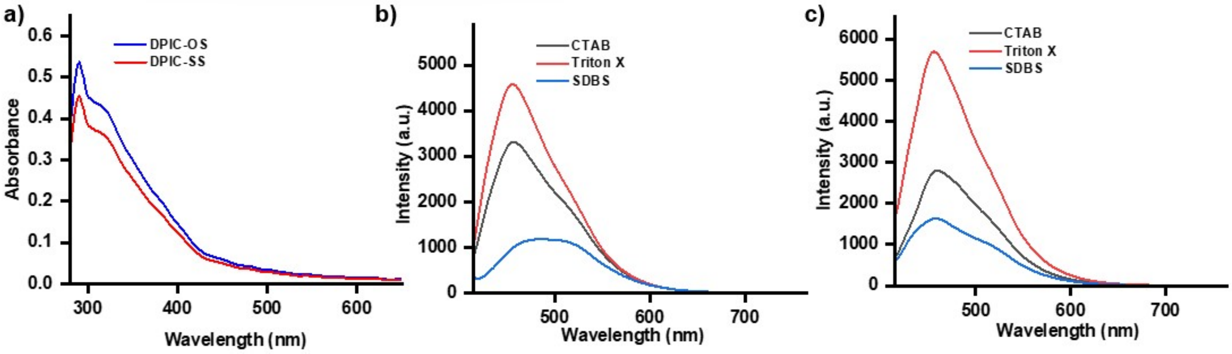

Figure S2. a) The absorbance of **DPIC-OS** and **DPIC-SS** in micellar media (CTAB, 1mM). The flourescence responses of b) **DPIC-OS** (10 µM) and c) **DPIC-S** (10 µM) in micellar media (λ_{ex} = 400 nm; λ_{em} = 455 nm, 505 nm).

5. Table S2: Comparative photophysical studies of DPIC-OS and DPIC-SS in micellar media

DPIC-SS	**λ_{abs} (nm)**	**λ_{em} (nm)**	**Intensity**	**Stokes shift (nm)**	**ΔE (J)**	**φ**
CTAB	287	459	2874	172	1.16×10^{-18}	44
SDBS	275	453	1628	178	1.12×10^{-18}	32
Triton X-100	289	454	5698	165	1.20×10^{-18}	51

DPIC-OS	**λ_{abs} (nm)**	**λ_{em} (nm)**	**Intensity**	**Stokes shift (nm)**	**ΔE (J)**	**Φ**
CTAB	288	456	3318	168	1.18×10^{-18}	43
SDBS	275	454	1000	179	1.11×10^{-18}	35
Triton X-100	289	454	4589	165	1.20×10^{-18}	58

6. Fluorescence spectra of DPIC-SS and DPIC-OS in varying concentrations of CTAB

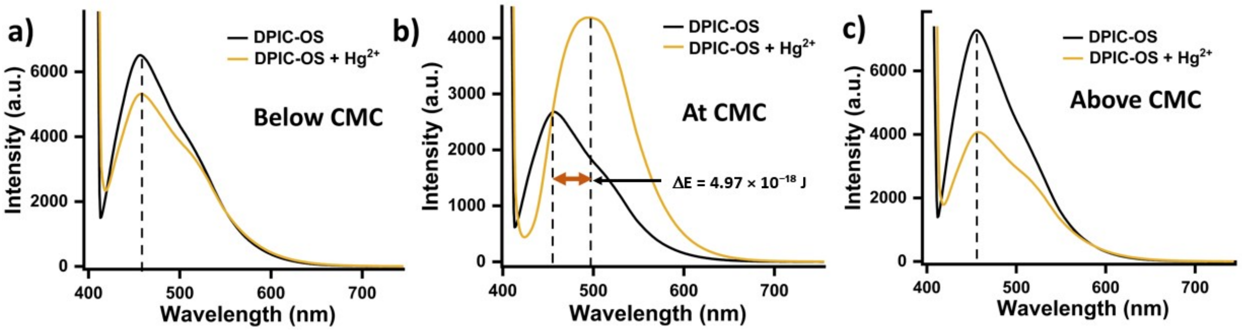

Figure S3. The fluorescence responses of **DPIC-OS** (10 µM) in aqueous solutions in the presence of varying concentrations of CTAB: a) 0.5 mM (below), b) 1 mM (around CMC) and c) 2 mM (much above CMC) (λ_{ex} = 400 nm; λ_{em} = 455 nm, 505 nm) [Note: The CMC of CTAB is 0.9 mM].

7. Time-dependent study for DPIC-OS and DPIC-SS upon addition of Hg^{2+}

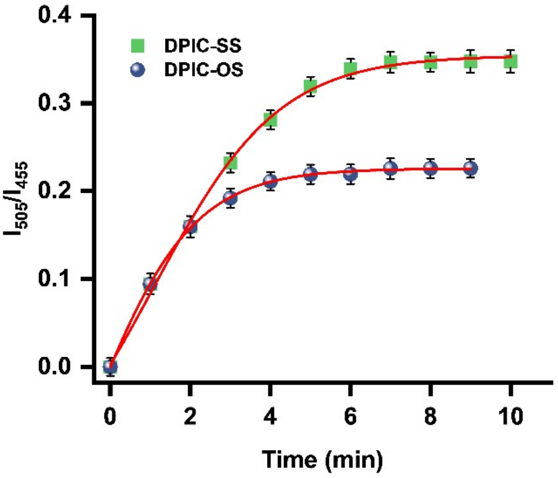

Figure S4. Time-dependent study and effect on the relative emission intensities of **DPIC-OS and DPIC-SS** (10 µM) upon addition of 25 µM of Hg^{2+} ions.

8. Fluorescence response of DPIC-CHO, DPIC-OS and DPIC-SS at different pH

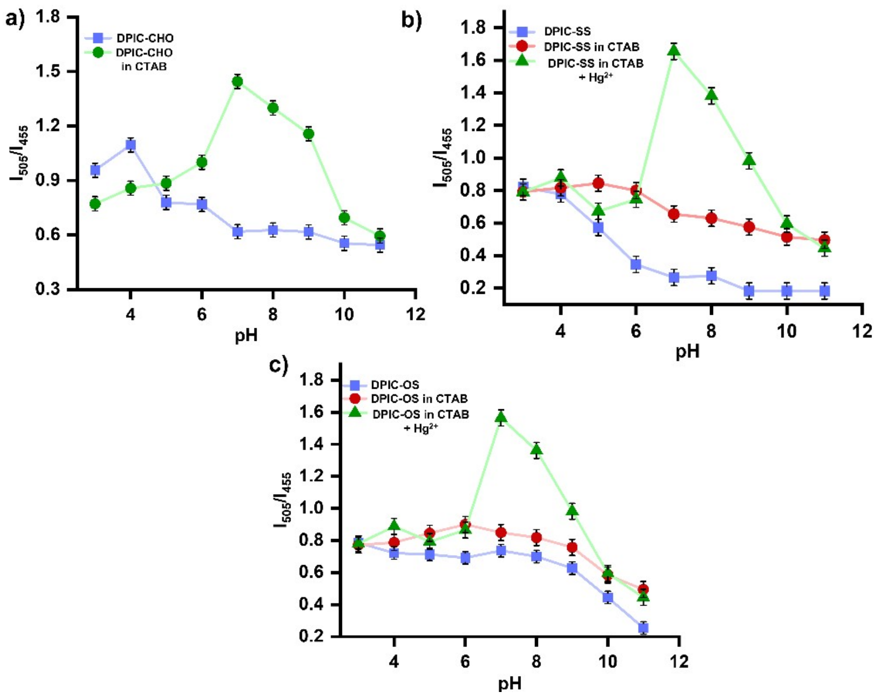

Figure S5. The fluorescence responses of **DPIC-SS**, **DPIC-OS** and **DPIC-CHO** in the presence and absence of Hg^{2+} ions as a function of pH with surfactant and without surfactant.

9. UV-Vis responses of DPIC-OS in the presence and absence of Hg^{2+} ions

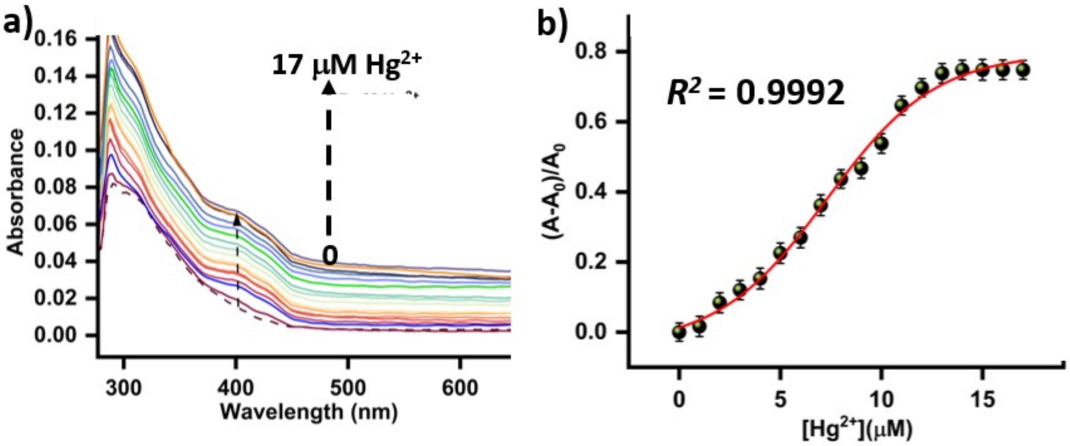

Figure S6. Colorimetric response of **DPIC-OS**: a) (20 μM in micellar solution in the presence of 1 mM CTAB) upon gradual addition of Hg^{2+} (0–17 μM). (b) Plot of the ratio of colorimetric response against Hg^{2+} concentrations (0–17 μM).

10. Table S3: Real sample analysis of DPIC-SS in the presence of Hg^{2+} ions

S. No.	Sample	Spiked concentration (μM)	Obtained concentration (μM)	%Recovery	RSD% n = 3
1	Rain Water	0.09	0.078	89	2.7
2	Tap Water	0.05	0.047	94	3.4
3	Pond Water	0.064	0.061	95	2.8
4	Distilled water	0.042	0.041	97	3.5
5	Sea Water	0.062	0.057	91	3.1
6	River Water	0.036	0.032	88	2.8

11. Table S4: Comparative table of selected hydrophobic fluorimetric probes for detection of Hg^{2+} ions via thioacetyl cleavage

Sr. No.	Probe Structure	Response time	Strategy	Media	Linear range (μM)	Detection limit (nM)	Real sample analysis	Ref.
1.	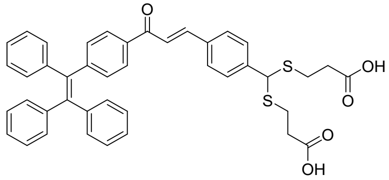 λ_{ex}= 395 nm; λ_{em} = 545 nm	4 s	thioether cleavage (turn-on via AIE)	MeOH/PBS (20 mM, pH = 7.4, 3:7, v/v)	4–14	416	food samples	[7]
2.	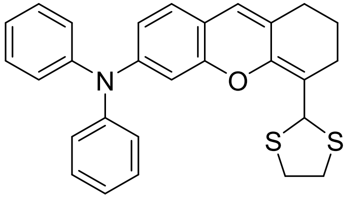 λ_{ex} = 440 nm; λ_{em} = 530 nm	4 min	thioacetal cleavage (turn-on)	THF/PBS (10.0 mM, pH 7.4, 7:3, v/v)	2–10	41.9	food samples	[8]
3.	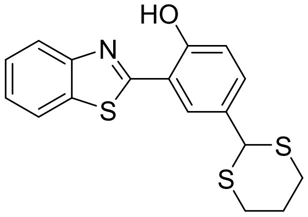 λ_{ex} = 514 nm; λ_{em} = 669 nm	30 min	ratiometric response	2% DMSO-PBS (pH = 7.4)	0–20	7.6	-	[9]

4.	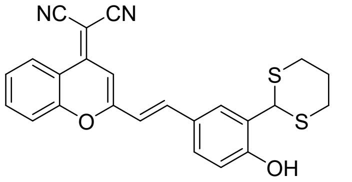 λ_{ex} = 514 nm; λ_{em} = 659 nm	-	thioacetal cleavage (turn-on)	DMSO:PBS (1:1)	0 –100	68	-	[10]
5.	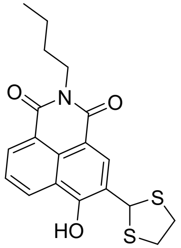 λ_{ex}= 414 nm; λ_{em} = 424 nm	10 min	deprotection reaction of the dithioacetal	0.01 M PBS (EtOH/water = 2:8 v/v; pH = 7.40)	0.25 – 10	40	water	[11]
6.	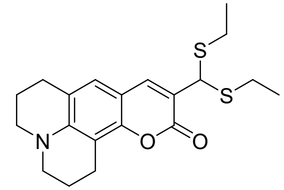 λ_{ex}= 395 nm; λ_{em1} = 440 nm λ_{em2} = 500 nm	-	thioether cleavage (ratiometric)	10% DMSO in HEPES	0–4	90	-	[12]
7.	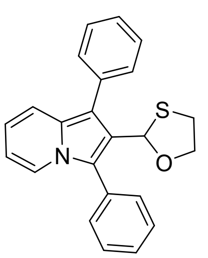 λ_{ex}= 400 nm; λ_{em1} = 455 nm λ_{em2} = 505 nm	2 min	thioacetyl cleavage (ratiometric)	CTAB 1mM	0–10	16.2	water samples	This work

12. Table S5: Comparative table of water-soluble fluorimetric probes for detection of Hg^{2+} ions

Sr.	Probe Structure	Response time	Media	Strategy	Linear range (µM)	Detection limit (nM)	Real sample analysis	Ref.
1.	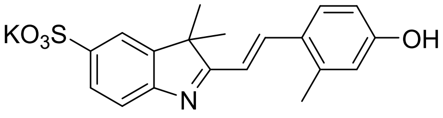 λ_{ex}= 378 nm; λ_{em} = 517nm	10 min	pure water	coordination	0 – 30	1.08×10^3	water	[13]
2.	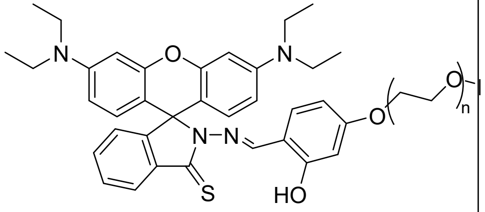 λ_{ex} 525 nm, λ_{em} 585 nm	1 h	NaOAc–HOAc buffer of pH 7.2	complexation	0.07 – 0.10	0.7	-	[14]
3.	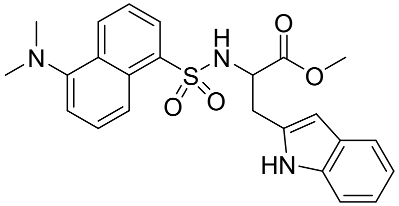 λ_{ex} 355 nm, λ_{em} 487 nm	15 min	10.0 mM HEPES solution (pH 7.5)	coordination	0 – 0.15	5.0	-	[15]

4.	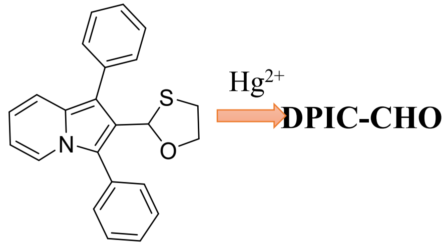 λ_{ex}= 400 nm; λ_{em} = 455 nm λ_{em} = 505 nm (**DPIC-CHO**)	2 min	1 mM CTAB	thioacetyl cleavage (ratiometric)	0-10	16.2	water samples	This work

13. References

[1]. Y. C. Yuan, T. Z. Liu, B. X. Zhao, Metal-free catalyzed synthesis of fluorescent indolizine derivatives, *J. Org. Chem.*, 2021, **86**, 12737-12744.

[2]. R. R. Parr, R. G. Yang, *Density functional theory of atoms and molecules*, Oxford University Press, New York, 1989 Search PubMed.

[3]. C. Jamorski, M. E. Casida, D. R. Salahub, Dynamic polarizabilities and excitation spectra from a molecular implementation of time-dependent density-functional response theory: N_2 as a case study, *J. Phys. Chem.,* 1996, **104**, 5134–5147.

[4]. R. Bauerschmitt, R. Alrichs, Treatment of electronic excitations within the adiabatic approximation of time dependent density functional theory, *Chem. Phys. Lett.,* 1996, **256**, 454–464.

[5]. R. Bauerschmitt, M. Häser, O. Treutler, R. Alrichs, Calculation of excitation energies within time-dependent density functional theory using auxiliary basis set expansions*, Chem. Phys. Lett.,* 1997, **264**, 573–578.

[6]. M. J. Frisch, G. W. Trucks, H. B. Schlegel, G. E. Scuseria, M. A. Robb, J. R. Cheeseman, J. A. Montgomery Jr, T. Vreven, K. N. Kudin, J. C. Burant, J. M. Millam, S. S. Iyengar, J. Tomasi, V. Barone, B. Mennucci, M. Cossi, G. Scalmani, N. Rega, G. A. Petersson, H. Nakatsuji, M. Hada, M. Ehara, K. Toyota, R. Fukuda, J. Hasegawa, M. Ishida, T. Nakajima, Y. Honda, O. Kitao, H. Nakai, M. Klene, X. Li, J. E. Knox, H. P. Hratchian, J. B. Cross, V. Bakken, C. Adamo, J. Jaramillo, R. Gomperts, R. E. Stratmann, O. Yazyev, A. J. Austin, R. Cammi, C. Pomelli, J. W. Ochterski, P. Y. Ayala, K. Morokuma, G. A. Voth, P. Salvador, J. J. Dannenberg, V. G. Zakrzewski, S. Dapprich, A. D. Daniels, M. C. Strain, O. Farkas, D. K. Malick, A. D. Rabuck, K. Raghavachari, J. B. Foresman, J. V. Ortiz, Q. Cui, A. G. Baboul, S. Clifford, J. Cioslowski, B. B. Stefanov, G. Liu, A. Liashenko, P. Piskorz, I. Komaromi, R. L. Martin, D. J. Fox, T. Keith, M. A. Al-Laham, C. Y. Peng, A. Nanayakkara, M. Challacombe, P. M. W. Gill, B. Johnson, W. Chen, M. W. Wong, C. Gonzalez, J. A. Pople, Gaussian 03, Revision E.01, Gaussian, Inc., Wallingford, CT, 2004

[7]. L. Tang, H. Yu, K. Zhong, X. Gao, J. Li, An aggregation-induced emission-based fluorescence turn-on probe for Hg^{2+} and its application to detect Hg^{2+} in food samples, *RSC Adv.*, 2019, **9**, 23316-23323.

[8]. S. Erdemir, S. Malkondu, A switch-on xanthene-triphenylamine based fluorescent and colorimetric sensor for the detection of ultra-trace Hg^{2+} in food samples and living cells. *Food Chem.*, 2022, **376**, 131951.

[9]. B. Gu, L. Huang, W. Su, X. Duan, H. Li, S. Yao, A benzothiazole-based fluorescent probe for distinguishing and bioimaging of Hg^{2+} and Cu^{2+}. *Anal. Chim. Acta*, 2017, **954**, 97-104.

[10]. L. Huang, Z. Yang, Z. Zhou, Y. Li, S. Tang, W. Xiao, H. Li, A dual colorimetric and near-infrared fluorescent turn-on probe for Hg^{2+} detection and its applications. *Dyes Pigm.*, 2019, **163**, 118-125.

[11]. M. Tian, C. Wang, Q. Ma, Y. Bai, J. Sun, C. Ding, A highly selective fluorescent probe for Hg^{2+} based on a 1, 8-naphthalimide derivative. *Acs Omega*, 2020, **5**, 18176-18184.

[12]. X. Cheng, S. Qu, L. Xiao, W. Li, P. He, Thioacetalized coumarin-based fluorescent probe for mercury (II): ratiometric response, high selectivity and successful bioimaging application. *J. Photochem. Photobiol., A*, 2018, **364**, 503-509.

[13]. Y. Zhang, C. Zhang, Y. Wu, B. Zhao, L. Wang, B. Song, A novel water-soluble naked-eye probe with a large Stokes shift for selective optical sensing of Hg^{2+} and its application in water samples and living cells. *RSC Adv.*, 2019, **9**, 23382-23389.

[14]. S. Hazra, S. Balaji, M. Banerjee, A. Ganguly, N. N. Ghosh, A. Chatterjee, A PEGylated-rhodamine based sensor for "turn-on" fluorimetric and colorimetric detection of Hg^{2+} ions in aqueous media. *Anal. Methods*, 2014, **6**, 3784-3790

[15]. H. W. Li, Y. Li, Y. Q. Dang, L. J. Ma, Y. Wu, G. Hou, L. Wu, L. An easily prepared hypersensitive water-soluble fluorescent probe for mercury (II) ions. *Chem. Commun.*, 2009, **29**, 4453-4455.

14. NMR spectra

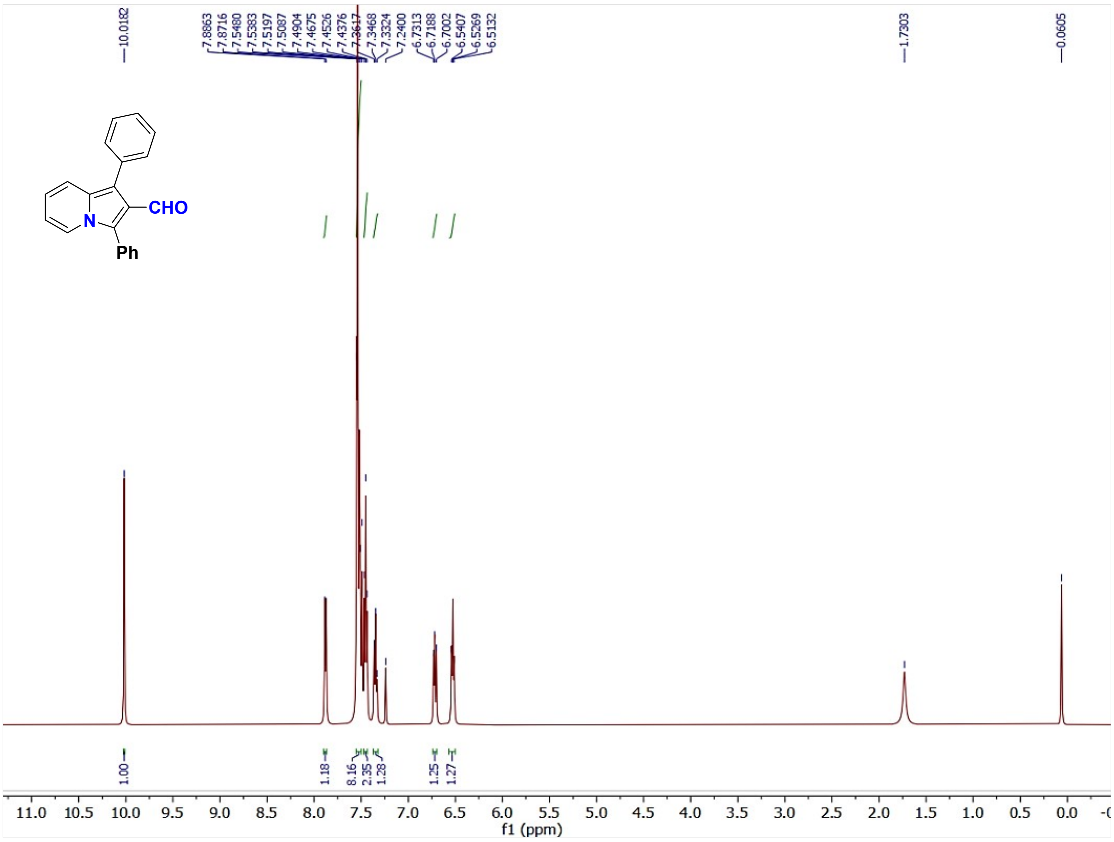

Figure S7. ^{1}H NMR spectrum of **DPIC-CHO** ($CDCl_3$, 500 MHz).

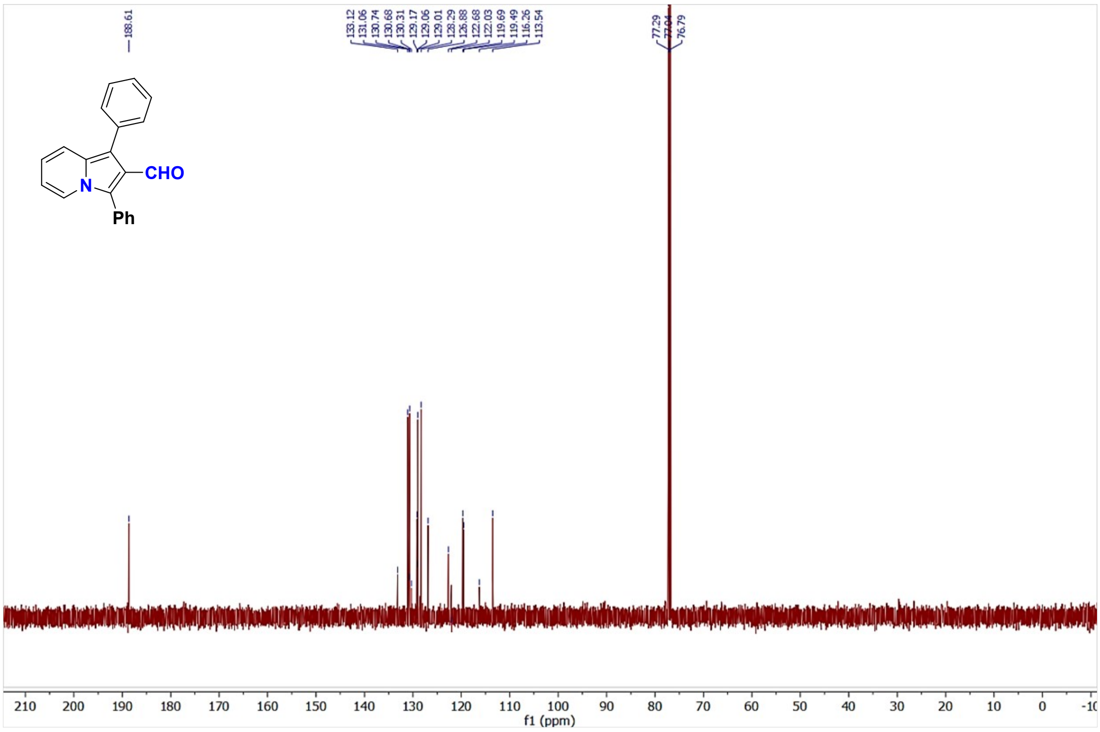

Figure S8. ^{13}C NMR spectrum of **DPIC-CHO** ($CDCl_3$, 125 MHz).

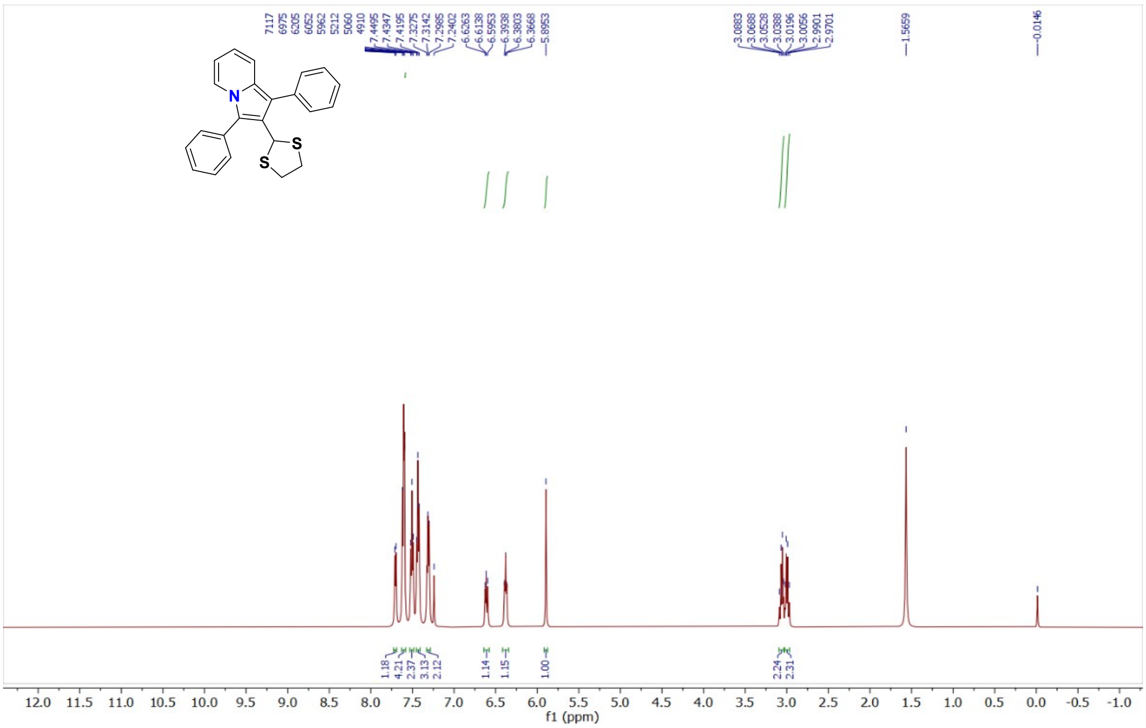

Figure S9: ^{1}H NMR Spectra of **DPIC-SS** ($CDCl_3$, 500 MHz)

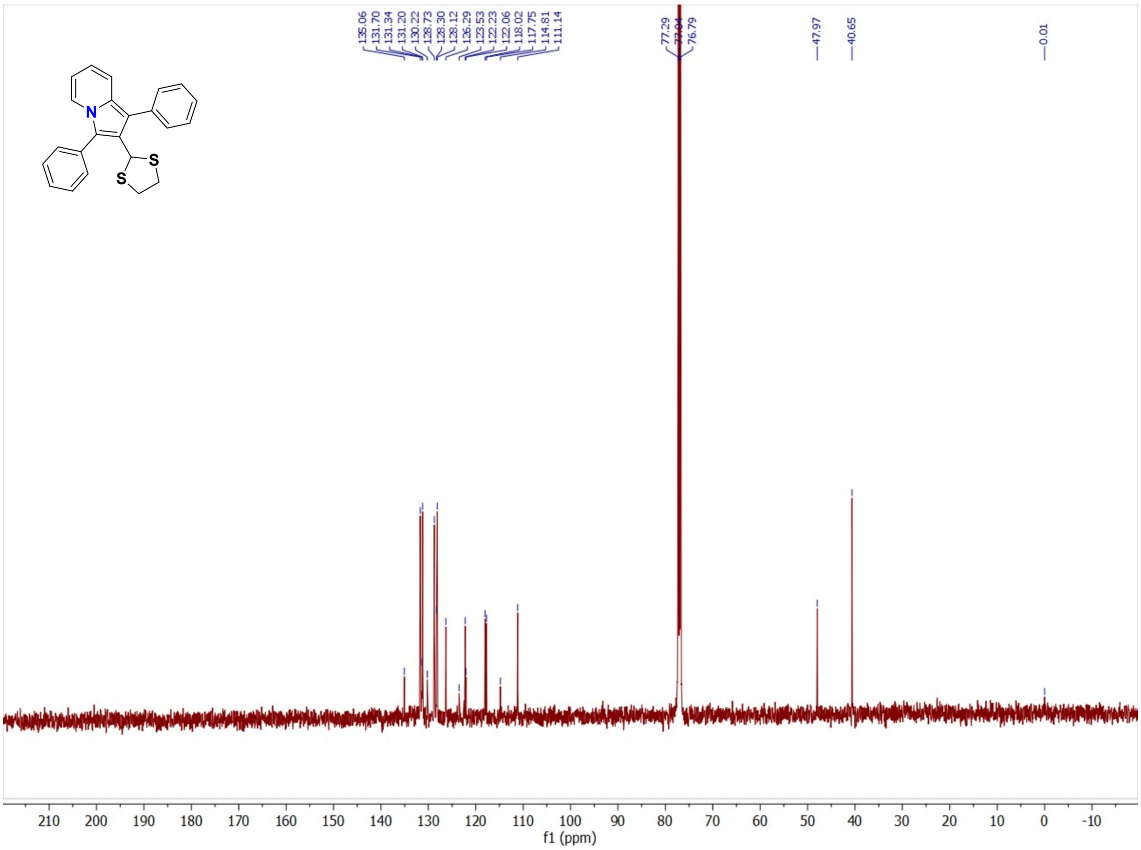

Figure S10. ^{13}C NMR Spectra of **DPIC-SS** ($CDCl_3$, 125 MHz)

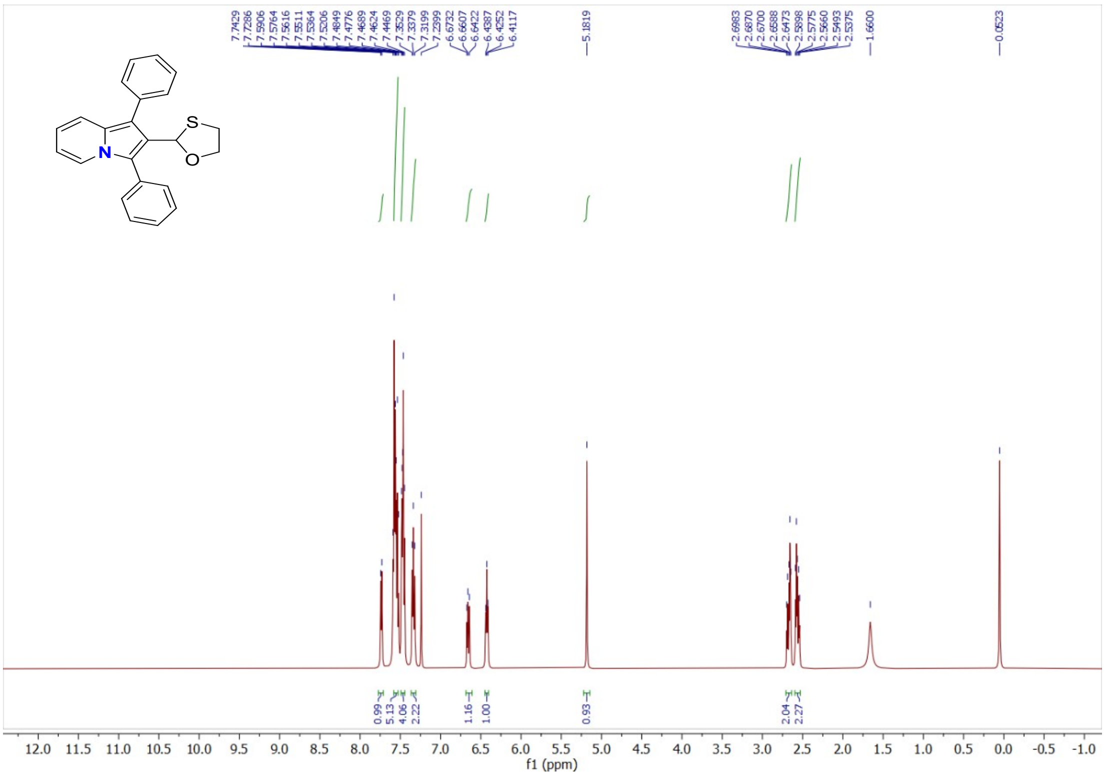

Figure S11: ^{1}H NMR Spectra of **DPIC-OS** ($CDCl_3$, 500 MHz)

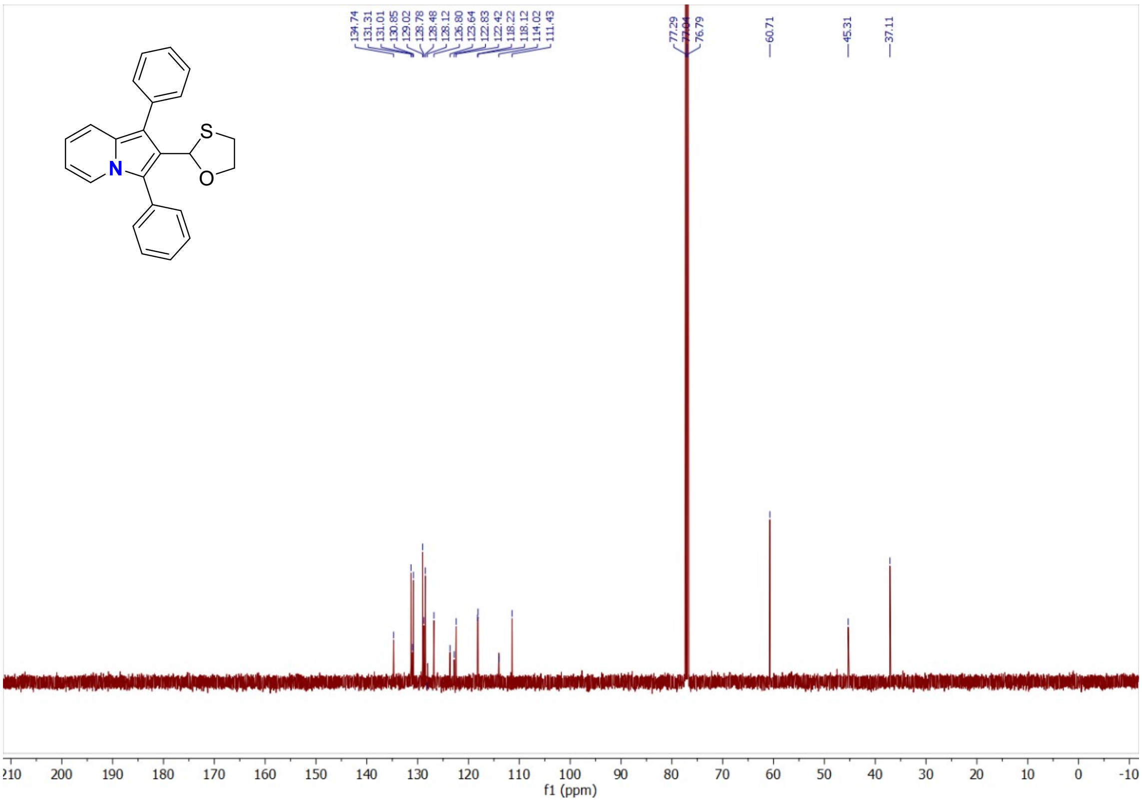

Figure S12. ^{13}C NMR Spectra of **DPIC-OS** ($CDCl_3$, 125 MHz)